Chemical Engineering Science, 1966, Vol. 21, pp. 975–997. Pergamon Press Ltd., Oxford. Printed in Great Britain.

An approximate theory for pressures and arching in hoppers

D. M. WALKER

Central Electricity Generating Board, S.W. Region R. & D. Laboratories, Portishead, Bristol

(*First received* 6 *December* 1965; *in revised form* 18 *April* 1966)

Abstract—A simple theory is developed which yields the approximate stresses within a granular material or powder flowing in hopper systems and gives the critical factors which ensure continued gravity flow.

The stress fields during mass flow have been derived by consideration of the forces acting on elemental slices which are simultaneously yielding within themselves and along the hopper walls.

Like Jenike, who has given an exact stress solution for hopper outlets only, when considering arching it is assumed that the powder strength is a function only of the local stresses that prevailed during the preceeding flow. Allowance has now been made, however, for the effect of the limited vertical shear stress that can be developed near a steep smooth wall on potential arch span. Consequently, the ideal hopper, designed from the material strength–stress characteristics is likely to have steep smooth walls which get steeper towards the outlet.

1. INTRODUCTION

THE DIFFICULTIES experienced in getting wet fine coal to flow through bunkers, hoppers and chutes has given rise to this theoretical investigation into the mechanics of the gravity flow of cohesive granular materials.

A granular material or powder, unlike a liquid, can support static shear stresses. A cohesive granular material can further support a static stress system with one stress-free surface and is thus capable of forming a self-supporting obstruction to flow.

The approach adopted to obtain design data for bunker flow is basically similar to that adopted by JENIKE [1], in that it comprises the study of the three relationships involving strength, stress and span:—

(a) *Strength–stress relationship*

A powder develops a strength according to the stresses at which it has been shear-consolidated. Strength–stress characteristics for coal powders have been measured using a Jenike shear cell and our own annular ring shear cell.

(b) *Stress–span relationship*

The consolidating stresses to be expected at any level within a powder in a bunker (or chute) during mass flow are derived theoretically and are now being measured experimentally.

(c) *Span–strength relationship*

The maximum potential arch spans are derived theoretically by comparing the stresses in self-supporting arches with the strength of the powder found in (a) at consolidating stresses derived in (b).

This paper first briefly explains the powder characteristics being tested in (a), details of which will be published later, and then covers the derivation of new theories for (b) and (c).

2. THE MOHR CIRCLE AND POWDER YIELD LOCI

The stresses at any point in a powder can be represented by three mutually perpendicular principal stresses. Only compressive stresses are considered (because the tensile strength of the powders concerned is very small) and it is assumed that the largest and smallest of the three will decide whether the powder compact will fail and flow, independently of the intermediate principal stress.

Considering a cross-section perpendicular to

both the major and minor principal planes (as shown in Fig. 1(a), then a Mohr circle represents the shear and compressive stresses on planes at all angles with the major principal plane. This is derived in texts on theoretical soil mechanics [TERZAGHI [2]).

The strength of a powder, prepared to a specific degree of consolidation can be represented on the shear–compressive stress diagram by a yield locus. This is shown in Fig. 2 together with a wall-yield locus which represents the limiting stress conditions which can be sustained at a plane wall of solid material bounding the powder.

If the stresses in one part of the powder are represented by a Mohr circle lying completely below the powder yield locus, such as that shown with centre at C_1, then the powder will remain at rest unless the part of the powder being considered is adjacent to a wall and the point representing the plane of the wall lies at D or E, in which case the powder will slip along the wall. If the wall plane is represented by a point on the circle lying below D or E no wall slip will occur.

For a powder in the state of plastic equilibrium on the point of plastic yield (or flow), then the Mohr circle representing the stress conditions must touch the powder yield locus. The circle with centre at C_2 is such a circle and point F represents the failure plane.

For a real cohesive powder there exists a whole family of yield loci corresponding to different consolidations (see Fig. 3), each locus terminating at the stress conditions appropriate to its consolidation (it cannot be subjected to higher stresses without becoming further consolidated). The envelope of the terminal Mohr circles of the individual yield loci, is termed the "effective Yield Locus" and this represents the shear-compressive stress characteristics of a powder consolidated under the same stress conditions at which it is being sheared, i.e. under the equilibrium conditions reached during a steady state of flow. The powder is then said to be in a "critical state".

Even for a cohesive powder it is found experimentally that the effective yield locus is approximately linear and passes through the origin, as is

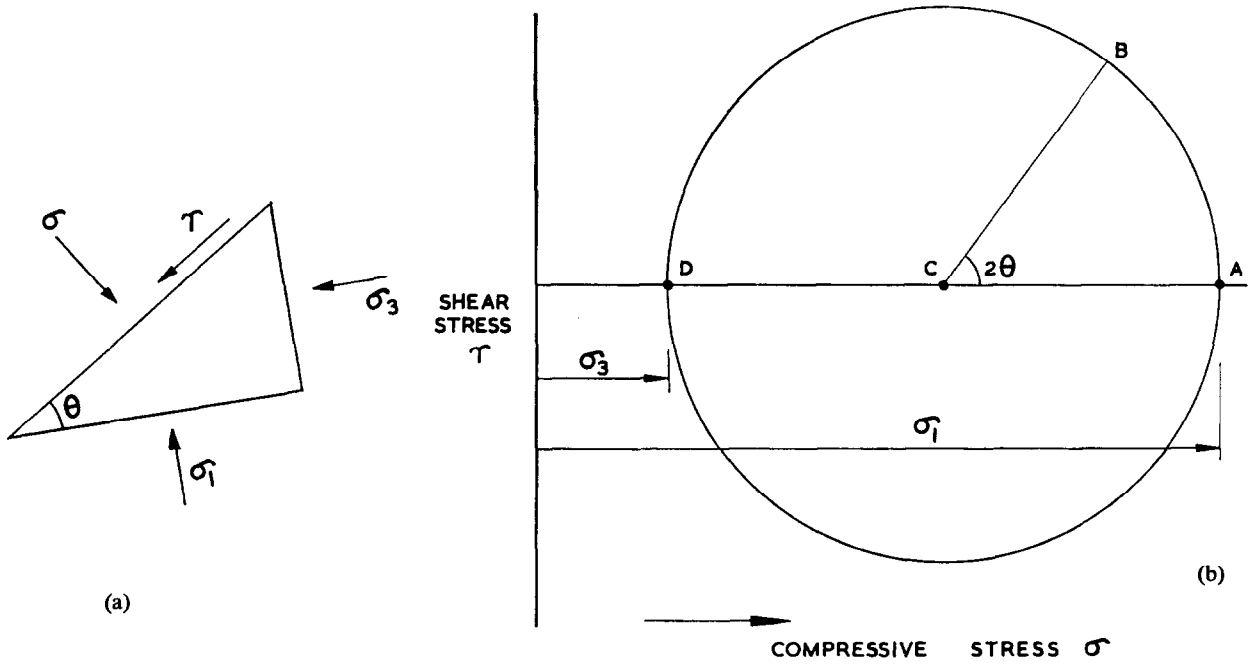

FIG. 1. The Mohr circle. A represents the major principal plane, compressive stress σ_1. D represents the minor principal plane, compressive stress σ_3. B represents a plane making an angle θ with the major principal plane. Angle BCA in the Mohr circle diagram is 2θ.

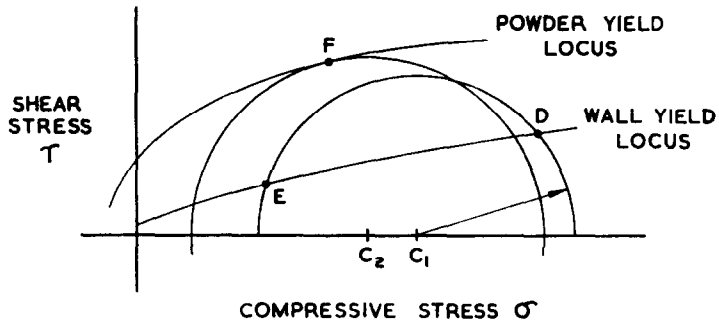

FIG. 2. Yield loci and Mohr circles.

the wall yield locus (providing the stress region being considered is not so low that wall adhesion, about 0·1 lb/in^2 for wet coal on stainless steel, is significant). Angle δ (Fig. 3) is termed the effective angle of friction whilst angle ϕ is the angle of wall friction. The effective yield locus appears to be the "critical state line" of ROSCOE, SCHOFIELD and WROTH [3], which was found to be linear through the origin, in the (τ, σ) system of co-ordinates, for saturated clays and closely graded cohesionless materials.

During mass flow in a convergent channel (considered later) it is the *effective* yield locus that is used (as by JENIKE [1]) in deciding the stress field. It can be argued that the constantly shearing powder is only consolidated to an extent appropriate to the actual shearing stresses at any moment—even when moving from high to lower stress fields the constant shearing destroys over-consolidation and maintains a "critical state" condition. When, however, the strength of the potential arch across the outlet is considered then the *individual* yield loci are relevant since now the powder, which has been consolidated during flow, is tested for its static strength.

3. POWDER STRENGTH AND CONSOLIDATION (THE STRENGTH–STRESS RELATIONSHIP)

A powder characteristic which decides whether it can resist flow under gravity from a certain bunker configuration is its unconfined yield strength (f), which is, of course, a function of the consolidating stress (σ_1) present during its preparation.†

$$\text{flowfactor } FF = \frac{\sigma_1}{f} \tag{1}$$

† A low unconfined yield strength for a given consolidation would naturally indicate a free flowing material. The ratio σ_1/f will thus be some measure of material flowability and, after Jenike it is called the flowfactor FF.

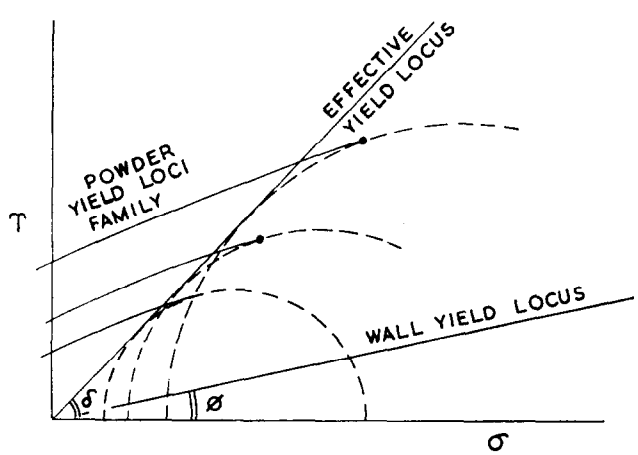

FIG. 3. Effective yield locus.

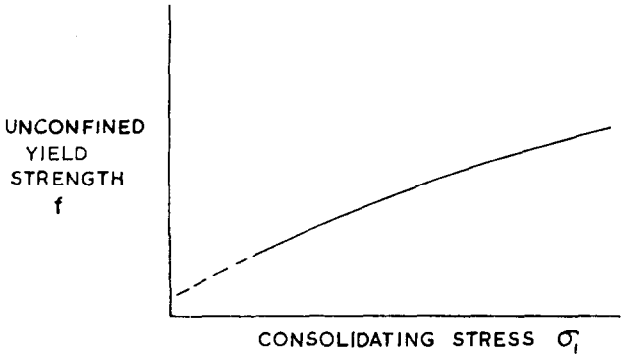

FIG. 4. The strength–stress characteristic.

A high value of *FF* would indicate a free flowing material with comparatively low unconfined yield strength, whilst a low value of *FF* would indicate a very cohesive, poorly flowing material.

In practice it is found that the value of *FF* for a given material varies with σ_1 and the f vs. σ_1 characteristic of a typical material is shown in Fig. 4. Here the flowfactor improves with increasing σ_1.

A Jenike shear cell has been used to find material characteristics and currently our own annular ring shear cell is being tried. In these tests a specimen is prepared by shear-consolidating it to a critical state under a given normal load and then tested for shear strength under another smaller normal load. From a set of such tests a yield locus of shear strength against normal load is plotted as shown in Fig. 5.

From this yield locus, f is obtained by drawing a circle through the origin with the yield locus as a tangent and σ_1 by drawing a circle such that the yield locus is tangent to it at the top locus point. (Circle centres to be on the $\tau = 0$ axis.) This set of tests locates one point on the flowfactor curve and must be repeated at other consolidating loads to locate the whole flowfactor curve.

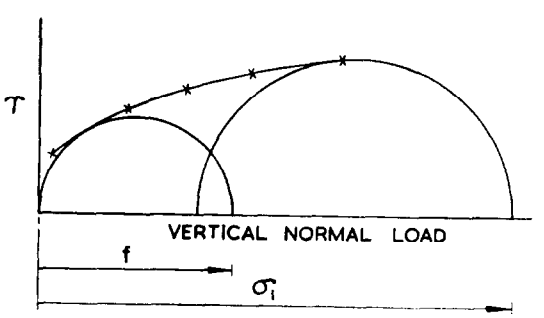

FIG. 5. Shear–normal load yield characteristic.

4. STRESS FIELDS (THE STRESS–SPAN RELATIONSHIP)

4.1 *Vertical pipe*

When material is loaded into a vertical pipe (or parallel-sided chute) the vertical pressure on any horizontal element tends initially to be the major principal stress, which as it builds up, causes the element to continually fail outwards towards the wall maintaining a horizontal reaction from the wall just sufficiently high to restore static plastic equilibrium. These stress conditions at any level in the material are taken to approximate to those represented by a Mohr circle just touching the effective powder yield locus, although this strictly depends on the powder having flowed enough to be in the critical state.

In practice as material is fed into the pipe it will compress the material already in the pipe which will subside and fully mobilise the wall friction. This will distort the stress field in such a way that the stresses in material adjacent to the wall and those in material at the centre of the same horizontal element must be represented by two Mohr circles such as the pair shown in Fig. 6. There is no shear stress along the pipe axis (from symmetry) and the horizontal stress remains the minor principal stress (point Q). On the wall, however, we assume the normal stress to be still equal to the same horizontal stress (H) but it is no longer the minor principal stress because wall friction has

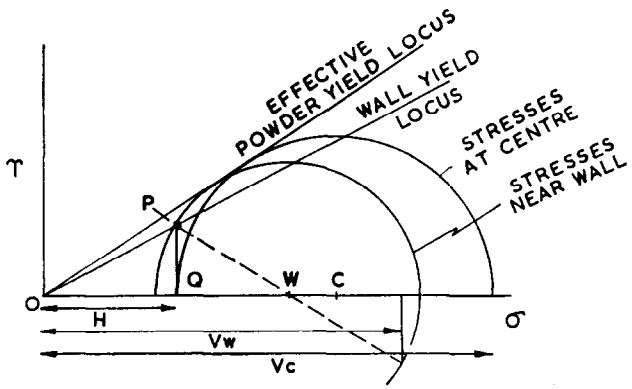

FIG. 6. Stress conditions in vertical pipe.

introduced a vertical shear stress. Point P represents the stresses on the wall being on the wall yield locus vertically above Q in Fig. 6. Mohr circles passing through P and Q and touching the effective powder yield locus represent the complete stresses at the wall and centre (respectively) of the element slice. The vertical stress at the centre (V_c) is greater than the vertical stress (V_w) at the wall, and the average vertical stress over the slice will be somewhere the two values.

Let

$$V_w = D\bar{V} \tag{2}$$

where $\bar{V}$ = average vertical stress on element slice
V_w = vertical stress near wall.

D we can call the "distribution factor" which would be a function (discussed later) of δ and ϕ, but is assumed to be a constant for any given system.

To obtain the average vertical stress as a function of depth we now consider the vertical forces acting on a thin horizontal elemental slice thickness dh, and distance h below the free surface in a vertical pipe of radius R. The formulae will also be applicable to vertical chutes of other cross-sectional shapes if twice the area to perimeter ratio is substituted for R. Resolving the vertical forces on the element slice

Weight = Vertical pressure difference force plus wall shear resistance force.

$$\gamma\pi R^2 dh = \pi R^2 d \quad + 2\pi R\tau_v dh$$

or

$$\frac{d\bar{V}}{dh} = \gamma - \frac{2\tau_v}{R} \tag{3}$$

Now τ_v can be related to V_w (and thus to $\bar{V}$) by considering the Mohr circle, Fig. 7.

From $\triangle OPW$

$$\frac{PW}{\sin\phi} = \frac{OW}{\sin i}, \text{ and } \varepsilon = \phi + i$$

but $PW = r$ and $OW = r/\sin\delta$

$$\therefore\ i = \arcsin\frac{\sin\phi}{\sin\delta}$$

$$\therefore\ \varepsilon = \phi + \arcsin\frac{\sin\phi}{\sin\delta}$$

(the arcsin to be >90°) (4)

$$\tau_v = PQ = r\sin\varepsilon$$

and

$$V_w = OT = OW + WT = r/\sin\delta + r\cos\widehat{TWS}$$
$$= r/\sin\delta - r\cos\varepsilon$$

Let

$$\tau_v = BV_w \tag{5}$$

where

$$\therefore B = \frac{\sin\varepsilon\sin\delta}{1 - \cos\varepsilon\sin\delta} \tag{6}$$

B is then a function of ϕ and δ (the friction angles) only and is a constant for any one system. From

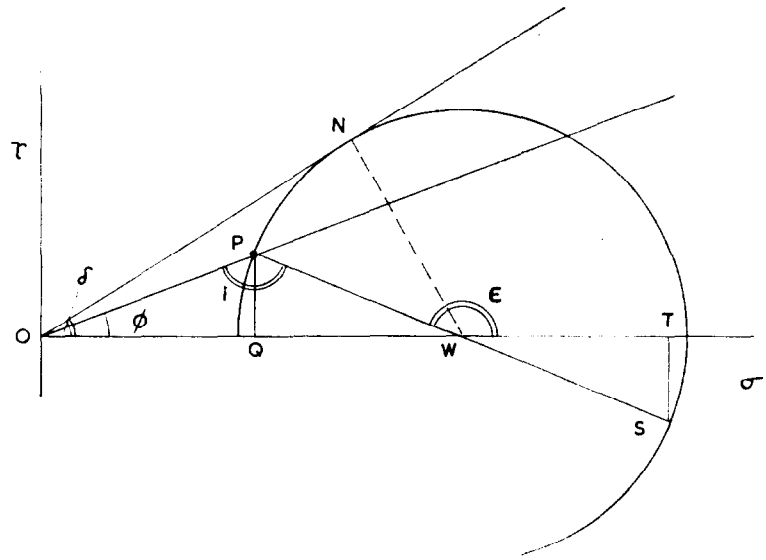

FIG. 7. Mohr circle for material near pipe wall.

(2), (3) and (5)

$$\frac{d\bar{V}}{dh} = \gamma - \frac{2BD}{R}\bar{V} \tag{7}$$

the solution of which, since $\bar{V} = 0$ when $h = 0$ is

$$\bar{V} = \frac{R\gamma}{2BD}\left(1 - \exp\left(\frac{-2BDh}{R}\right)\right) \tag{8}$$

The corresponding horizontal pressure H at depth h is, since $\tau_v/H = \tan\phi$ (wall friction) and $\tau_v = BV_w$,

$$H = \frac{BV_w}{\tan\phi} = \frac{BD\bar{V}}{\tan\phi}$$

$$\therefore H = \frac{R\gamma}{2\tan\phi}\left(1 - \exp\left(\frac{-2BDh}{R}\right)\right) \tag{9}$$

The only unknown in Eqs. (7) and (8) is D, the distribution factor, although this appears to be approximately equal to unity for all but very rough walled pipes. Actual values of D have been calculated for a circular pipe when the slice elements considered are far enough below the free surface for the average vertical stress to be taken as having reached equilibrium. In this case the weight of material within any cylindrical element (co-axial with pipe) must be equal to the shear force on the element's vertical cylindrical surface. This weight is proportional to the square of the element radius, and the surface is proportional to that radius; so the vertical shear stress must also be proportional to the radius. Values of D calculated on this basis are found to be only slightly less than unity until ϕ approaches δ when the value then drops to about 0·6.

Equations (8) and (9) are of similar exponential form to the classical Janssen equations except that we now have a factor BD instead of the nK in the original form, where $n = \tan\phi$ and K usually taken as being equal to $\frac{1 - \sin\delta}{1 + \sin\delta}$. For all but the rougher walled pipes BD is practically equal to nK, and D is practically equal to unity (see Table 1). For the rough walled pipes BD is slightly larger than nK and so gives lower average vertical pressures and higher horizontal pressures at all depths although the horizontal pressure tends to the same maximum with increasing depth.

It is of interest to note that in the case of a rough walled pipe we would expect the ratio of horizontal to vertical pressure near the wall to be $\frac{1 - \sin^2\delta}{1 + \sin^2\delta}$ instead of the classical soil mechanics ratio of $\frac{1 - \sin\delta}{1 + \sin\delta}$.

Table 1. *Constants for vertical pipes*
(*For a material* $\delta = 50°$)

Friction angle (ϕ)	ε	B	D	BD	*Usual Janssens* (nK)
0	180	0	1	0	0
5	178·5	0·011	0·998	0·011	0·012
10	177	0·022	0·996	0·022	0·023
20	173·5	0·05	0·9	0·049	0·048
30	169·25	0·08	0·97	0·078	0·077
40	164	0·12	0·93	0·112	0·111
45	157·6	0·17	0·86	0·146	0·133
50	140	0·31	0·61	0·189	0·158

If a surcharge pressure V_0 be imposed on the top surface of the material in the pipe (if for example it was joined beneath a hopper) then the pressures at various levels are again derived from Eq. (7) but with boundary condition $\bar{V} = V_0$ at $h = 0$. This gives, taking D as unity especially if V_0 is assumed to be a uniformly distributed pressure

$$\bar{V} = \frac{R\gamma}{2B}\left(1 - \exp\left(\frac{-2Bh}{R}\right)\right) + V_0 \exp\left(\frac{-2Bh}{R}\right) \tag{10}$$

and

$$H = \frac{B\bar{V}}{\tan\phi}$$

4.2 *Convergent hopper*

4.2.1 *Initial loading stresses.* The initial stress field set up on filling a convergent hopper is very different from the stress field set up once mass-flow discharge is under way. (See 4.2.3.)

As described in the vertical pipe case, on filling, the vertical pressure would tend to be the major principal stress which is continually built up with increasing head of material. It is now suggested that, if a hopper with reasonably smooth walls, at an angle α with the vertical, is filled with a practicably incompressible material, the stress field set up at any point near the walls would be as illustrated in Fig. 8.

The Mohr circle shown is one where point P on the wall yield locus is at an angle 2α around the circle from point Q. The circle, in the case of the reasonably smooth hoppers being considered, lies completely below the material's effective yield locus and no material yield takes place, except on the wall. The major principal stress direction remains vertical, and point Q represents the minor principal plane which is therefore also vertical. The stresses on the hopper wall, which is at an angle α with the vertical, are represented by point P.

During filling the vertical pressure will be building up: this will tend to inflate the circle and increase the wall stresses marginally above the wall yield locus. Slip on the wall will occur which will result in the horizontal stress increasing until the wall stresses are again on the wall yield locus. The

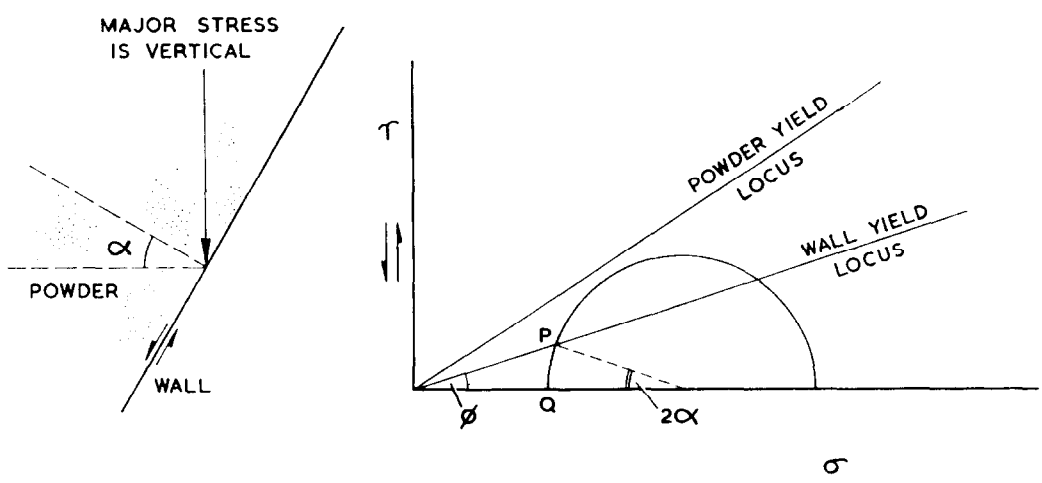

FIG. 8. Initial stress conditions at hopper wall.

stress circle will be continually increasing but the geometry should remain as shown in Fig. 8.

Since there is no shear stress on vertical planes, then the vertical pressure at any level is equivalent to the hydrostatic pressure due to the head of material above it. The wall pressure is a constant times the vertical pressure. From the geometry of Fig. 8

$$W = V \times \frac{\sin 2\alpha \cos \phi}{\sin(\phi + 2\alpha) + \sin \phi} \tag{11}$$

If the material is very compressible and large subsidences occur on filling, then the initial stress field is likely to be somewhere between that just described for a practially incompressible material and the stress field finally set up during mass flow discharge. If, however, a hopper is refilled after being partly emptied, then very high local wall stresses can be set up just below the original material level. These stresses are greater than those given in the other cases already mentioned, but will be similar to the case of a mass-flow field with a surcharge, dealt with later (Section 4.2.4).

4.2.2 *Mass and plug flow.* There can be two types of gravity flow from hoppers:

(a) *Mass flow*

In this case all the material is in motion and slip is occurring at the hopper walls. Mass flow is promoted by having the walls of the bunker sufficiently smooth and steep with no ledges, and is the only way of ensuring really continuous free flow from a hopper since otherwise the whole capacity of the hopper is not used and material is left to consolidate and possibly build up into obstructions.

(b) *Plug flow*

Here flow occurs within a pipe-shaped channel in the material itself. In the extreme case the pipe remains self-supporting and visible from above, but often material at the top of the hopper collapses and discharges in plug flow through a pipe within static material at the base of the hopper.

In the following sections the stresses occurring throughout the material during mass flow are derived. In later sections, conditions are found where the strength of the material, consolidated under these stresses, would just be capable of forming a static arch between the sides of the hopper.

4.2.3 *Stresses during mass flow.* During mass flow in a convergent hopper, it is assumed that:

(a) The major and minor principal stress directions are in the vertical plane normal to the nearest section of wall and these decide material yield independent of the third intermediate principal stress acting perpendicular to this plane.

(b) The material must be yielding within itself to enable it to pass through the reducing hopper cross-section. It is assumed that the material adjacent to the walls, at least, is not only in plastic equilibrium, but is also in the critical state appropriate to the local stresses during flow.

(c) The material must by definition of mass flow be slipping along the wall. The stresses on the wall are considered to be the larger of the two possible combinations because the material is virtually wedging itself into the hopper and will consequently promote the highest possible wall reactions compatible with material strength.

(d) In the simple case ($D = 1$) the vertical stress over a horizontal plane is taken to be constant. Variation of the vertical stress is considered and the effects of the consequent increased values of D shown to be small.

From the first two assumptions the stresses in the powder adjacent to the wall must be represented by a Mohr circle which just touches the powder yield locus OP (Fig. 9(b)) and from the third assumption the wall stresses must be represented by a point on the wall yield locus OW, and, in fact, point W (rather than point X).

Figure 9(a) illustrates the right-hand hopper wall at an angle α with the vertical, with the major principal stress direction at angle β with the wall-normal. The stresses on the various planes are then given as shown by the Mohr circle on Fig. 9(b), where M represents the major principal plane, W the wall and Y the vertical plane.

The angle β can be shown to be related to ϕ (the wall friction angle) and δ (the effective internal friction angle) in a similar manner as that followed for ε preceding Eq. (4).

$$\beta = \frac{1}{2}\left(\phi + \arcsin \frac{\sin \phi}{\sin \delta}\right) \tag{12}$$

The arcsin now to be less than 90° because we are concerned with point W rather than point X.

YR represents the shear stress on the vertical

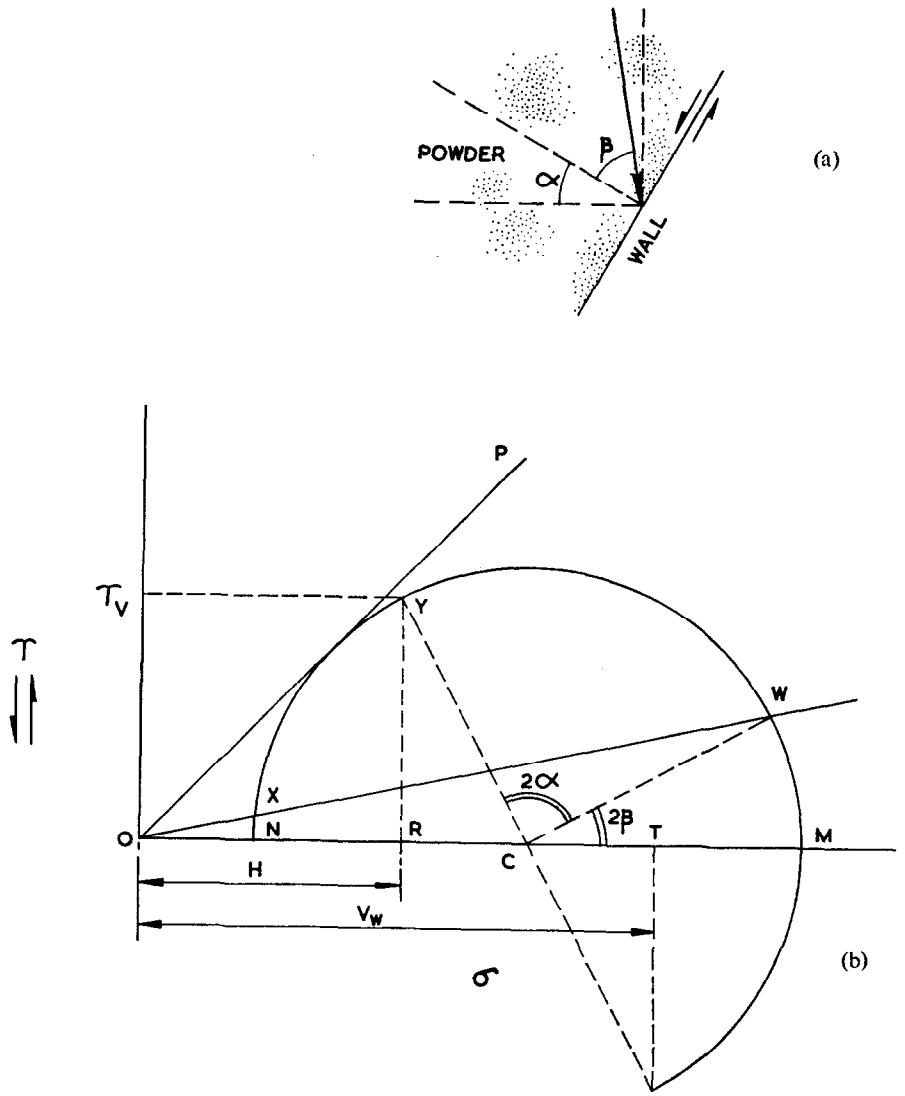

FIG. 9. Stress conditions developed at hopper wall.

plane (τ_v) whilst OR and OT represent the horizontal (H) and vertical compressive (V_w) stresses in the vicinity of the wall.

From the diagram, if r is circle radius

$$\tau_v = r \sin 2(\alpha + \beta)$$

$$V_w = OC + CT$$

$$\therefore V_w = \frac{r}{\sin \delta} - r \cos 2(\alpha + \beta)$$

let

$$\tau_v = BV_w \tag{13}$$

$$\therefore B = \frac{\sin \delta \sin 2(\alpha + \beta)}{1 - \sin \delta \cos 2(\alpha + \beta)} \tag{14}$$

Now we will require τ_v in terms of $\bar{V}$ (the average vertical stress over a horizontal section through the material) rather than V_w (the vertical stress in the vicinity of the wall).

Let

$$V_w = D\bar{V} \tag{15}$$

where D is unknown but assumed a constant for any one system. A simple case of taking D to be unity is shown later to be reasonably accurate.

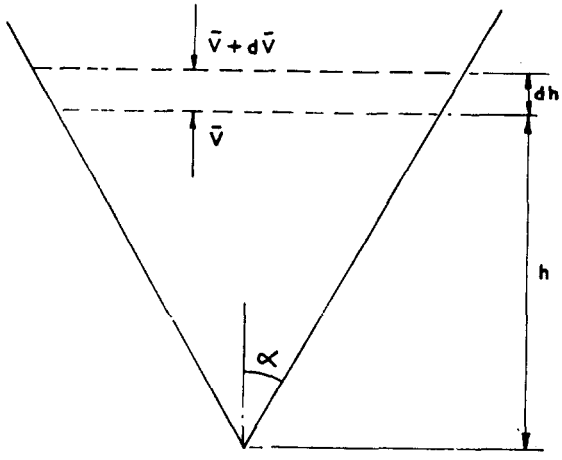

FIG. 10. Elemental slice in hopper.

Consider the forces on a horizontal element slice of material in a hopper, as in Fig. 10.

Stresses on elemental slice

Let P = perimeter of slice
A = area of slice
γ = bulk density.

Force balance

$$A\gamma dh + Ad\bar{V} = P\tau_v dh$$

Now from (13) and (15) $\tau_v = BD\bar{V}$

$$\therefore \frac{d\bar{V}}{dh} = \frac{P}{A} BD\bar{V} - \gamma \tag{16}$$

If it is a conical bunker, with circular cross-section radius R being considered

$$A = \pi R^2$$

$$P = 2\pi R$$

$$R = h \tan \alpha$$

$$\therefore \frac{d\bar{V}}{dh} = \frac{2BD\bar{V}}{h \tan \alpha} - \gamma$$

This also applies to a pyramidal hopper since P/A would be the same for the square cross-section as for the included circular. For a long wedge shape bunker (virtually two plane walls) then (16) becomes

$$\frac{d\bar{V}}{dh} = \frac{BD\bar{V}}{h \tan \alpha} - \gamma$$

Let

$$\frac{d\bar{V}}{dh} = C\frac{\bar{V}}{h} - \gamma \tag{17}$$

where $C = \dfrac{2BD}{\tan \alpha}$ for cone or pyramid, (18)

and $C = \dfrac{BD}{\tan \alpha}$ for wedge.

The average vertical pressure at any height (h) in a hopper filled to a height h_o (from apex) is found by integrating (17) and putting $\bar{V} = 0$ at $h = h_o$

$$\bar{V} = \frac{\gamma h}{C-1}\left(1 - \left(\frac{h}{h_o}\right)^{C-1}\right) \tag{19}$$

$$\left(\text{except when } C = 1, \text{ when } \bar{V} = \gamma h \log\left(\frac{h_o}{h}\right)\right)$$

LEE [4] proposed an equation similar to (17) and very recently [5] one equivalent to (19) to account for the shape of the pressure vs. depth curve obtained by JENIKE [6] in small hoppers. Lee however, is unable to compare C's (his symbol C is the reciprocal of that used here in Eq. (19)) for different hoppers without assuming that the vertical to horizontal pressure ratio in different hoppers is the same (apparently equal to $1 + \sin \delta / 1 - \sin \delta$). LENCZNER [7] also arrives at similar shaped pressure vs. depth curves but has to assume that the mobilised angle of friction of the contained material on a vertical plane is equal to the angle of wall friction. There is no apparent justification for either of these assumptions and they are very far from true in the present treatment.

The pattern of pressures given by Eq. (19) for different values of C is given in Fig. 11 whilst the values of C associated with different conical or pyramidal hoppers for the simple case ($D = 1$) is included in Table 2 which appears later.

For a given powder-hopper combination the vertical pressures developed during flow will be represented by one C value curve. This same curve will also represent the consolidating and wall stresses if the pressure scale is multiplied by the respective ratio represented in the Mohr circle (Fig. 9(b)).

The weakness of the present simple treatment is that D cannot be exactly evaluated. It can be seen, however, that providing D is not really much less

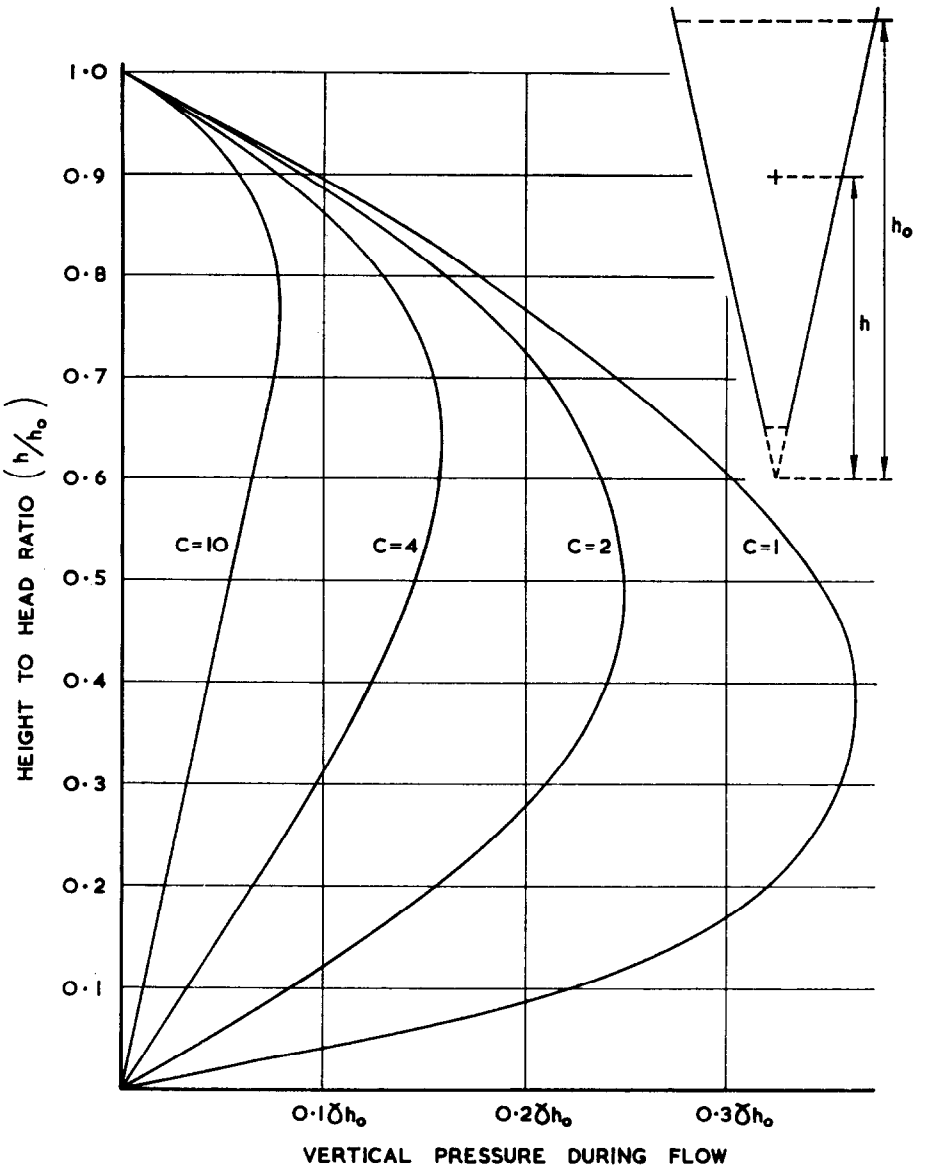

FIG. 11. Vertical pressures in hoppers.

than unity, then taking it to be unity (simple case) will give sufficiently accurate values of wall stresses, since these are derived from V_w and from (15) and (19)

$$V_w = D\bar{V} = \frac{D\gamma h}{C-1}\left(1-\left(\frac{h}{h_o}\right)^{C-1}\right) \qquad (20)$$

For values of $C \gg 1$ (which are given for the steeper smoother hoppers in the simple case), then the D in the numerator virtually cancels out the D contained in C in the denominator. Only the power term in (20) which mainly affects the less important stresses near the material free surface, remains dependent on the value of D.

That D is in fact not small compared with unity and therefore can be taken as unity in deriving wall pressures, is shown by

(a) some experimental vertical pressure measurements to be published later.

(b) a refinement of the simple theory on the basis

that the whole of the hopper fill is in plastic equilibrium condition and that on any horizontal plane only the horizontal stress is sensibly constant. The vertical shear stress drops from a value τ_v near the hopper wall to zero on the hopper axis. If it is assumed this drop is linear, values of D can be calculated to be between 1 and 2 for sensibly steep and smooth hoppers.

(c) the exact theory of JENIKE [1] applicable towards hopper outlets.

4.2.4 *Hopper with surcharge.* Consider the case of a hopper having a surcharge on its top surface, as in the case of a bunker comprising a vertical walled section on top of a convergent hopper section. The average vertical pressures are given again by integrating (17) but now putting at $h = h_o$, $\bar{V} = V_o$ (the surcharge pressure): this gives

$$\bar{V} = \frac{\gamma h}{C-1}\left(1 - \left(\frac{h_o}{h}\right)^{C-1}\right) + V_o\left(\frac{h}{h_0}\right)^C \quad (21)$$

For regions near the hopper outlet where $h \ll h_o$ (and taking $C > 1$ which will be so for mass flow) then both (19) and (21), the without and with surcharge cases, simplify to

$$\bar{V} = \frac{\gamma h}{C-1} \quad (22)$$

If R is the cross-section radius of a cone, or half the wall to wall span of a square pyramid or wedge, then, for the simple $D = 1$ case

$$V_w = \bar{V} = \frac{\gamma R}{\tan\alpha(C-1)}$$

then

$$\frac{V_w}{\gamma R} = \frac{1}{\tan\alpha(C-1)} = Y(\text{say}) \quad (23)$$

Now from Fig. 9(b), the major principal stress σ_1 (equal to OM in the figure) is related to V_w (equal to OT in figure) by

$$\frac{\sigma_1}{V_w} = \frac{1+\sin\delta}{1-\sin\delta\cos 2(\alpha+\beta)} = X\ (\text{say}) \quad (24)$$

This enables the major principal or consolidating stress near the hopper walls to be calculated from (19) or (21). Near the hopper outlet however

$$\frac{\sigma_1}{\gamma R} = XY \quad (25)$$

This expression will be used when "arching" criteria are considered.

Similarly wall normal stresses throughout a hopper can be obtained from Eqs. (19) or (21) for the simple case where $\bar{V} = V_w$, since from Fig. 9(b) it can be shown that the wall normal stress W (equal to the normal stress represented by point W in the figure) is related to V_w by

$$\frac{W}{V_w} = \frac{1+\sin\delta\cos 2\beta}{1-\sin\delta\cos 2(\alpha+\beta)} \quad (26)$$

4.3 *Experimental pressure measurements*

Experiments have been carried out with dry fine coal (pass $\frac{1}{32}$ in. sieve) in a small model bunker, shown in Fig. 12, and are currently being carried out with coal, pass $\frac{1}{8}$ in., in much larger experimental hoppers of up to 3 ton capacity. Wall pressures have been measured during very many discharge runs and vertical pressures during some of these runs. The wall pressures were measured by the slight deflections of stiff, flush diaphragms, and showed that the flow stress field was quickly developed from the initial stress field when only a small volume of coal had been discharged from the hopper base. The vertical pressures were measured in the small hopper by including, at one of the levels to be studied, a false horizontal platform which had a flexible rim and included one or two wall pressure probes. Lowering the platform appeared to promote approximately the same flow stress field, according to measured wall pressures, as conventional discharge from the base. On the large hoppers the vertical pressures are being measured by including mobile vertical facing diaphragm assemblies in the coal and assuming these remain still vertical over the small amount of flow required to promote the flow stress field. It is hoped to publish full details and results of these tests very soon. Some of the measured vertical and normal wall pressures developed during flow (Figs. 12 and 13) are shown here compared with those predicted by the present simple theory. Agreement is reasonably good.

Points plotted for the model bunker are averages for five runs, whilst the theoretical curves are cal-

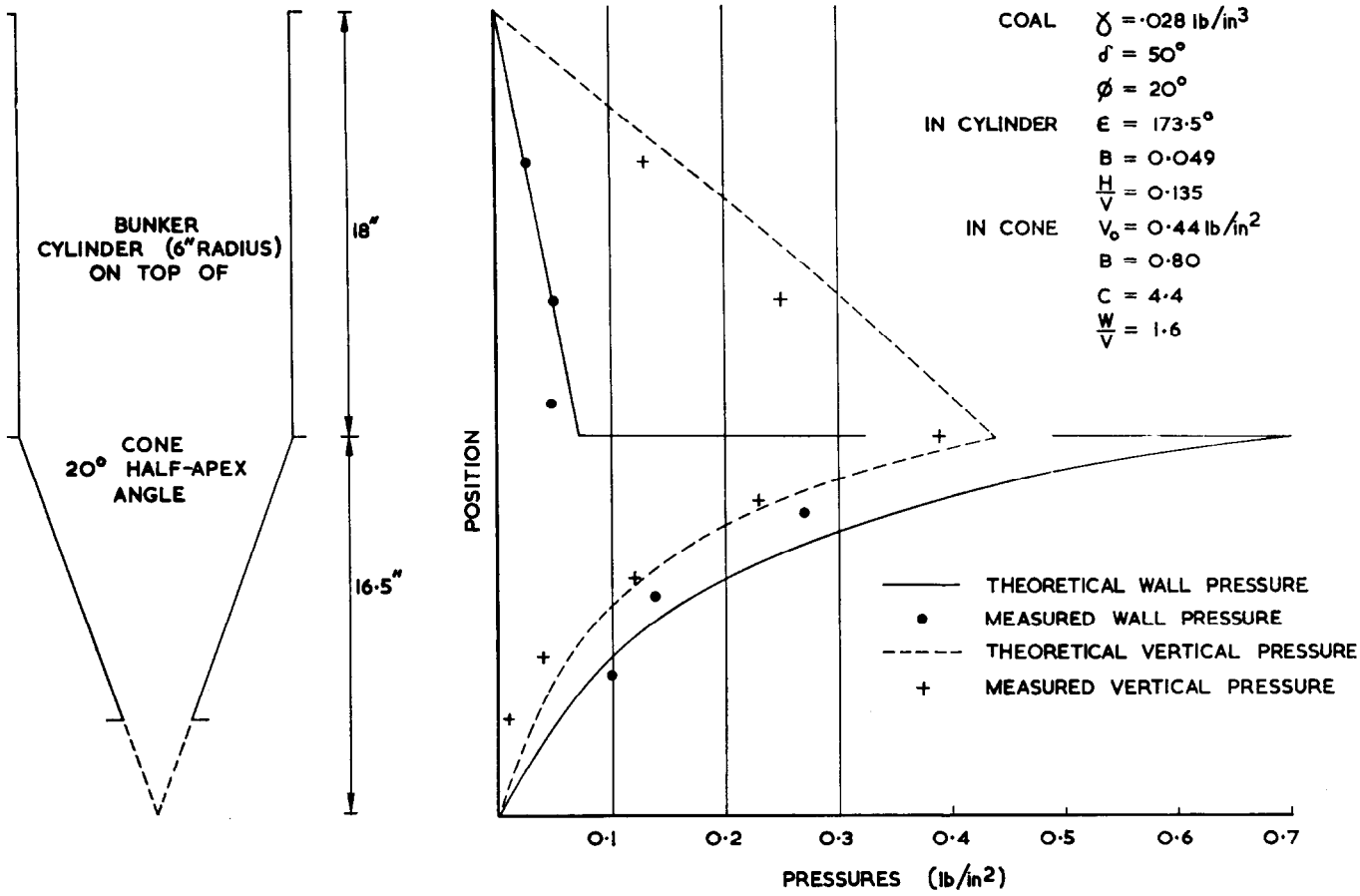

FIG. 12. Flow pressures in model bunker.

culated from (8) and (9) in the cylindrical section and (21) and (26) in the conical section. The shaded area for the larger hoppers covers the results of some thirty runs in the 15° half apex angle conical and square pyramidal hoppers (which were not significantly different). The theoretical curve is calculated from (19) and (26).

5. The Static Arch (The Span–Strength Relationship)

The situation considered in this section is where a free static arch is formed in a material which has previously been discharging from a mass flow hopper. During discharge, stress at any level in the lower part of the hopper has been shown to be proportional to span, and since material strength during flow is nearly proportional to stress, then the arched system is one where strength is nearly proportional to span. The simple concept of treating the blocked mass as made up of a stack of self-supporting element arches of similar basic shape, is applicable to this situation because the required strength for each unit arch is found (later in this section) to be proportional to span. The basic element arch can be taken as of uniform vertical thickness because this closely approximates to the requirement that the element shape, after appropriate scaling to bridge the hopper walls, should be capable of forming a stack of element arches one upon another, which then entirely accounts for the volume of material over the lower part of the hopper.

The arch stack is an extreme case taken for analysis. In practice, some way above the hopper outlet the material would have insufficient strength

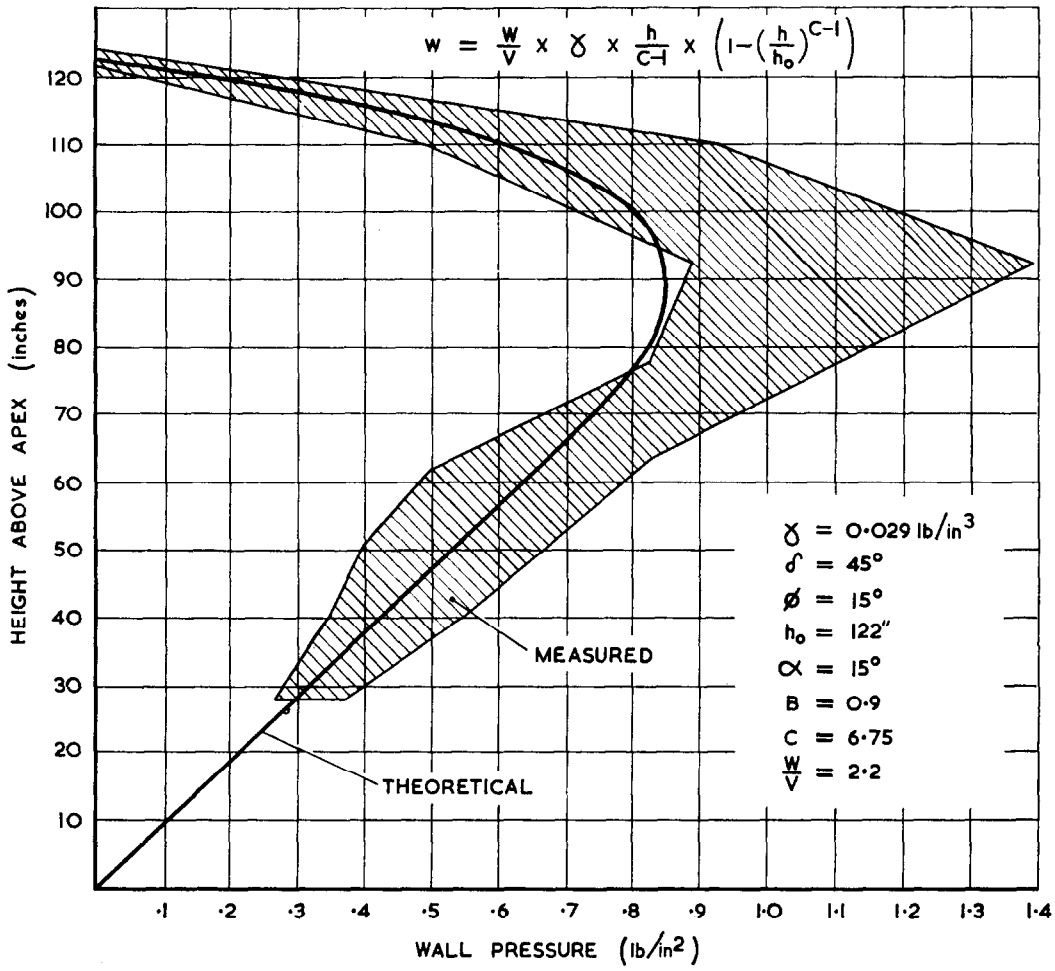

FIG. 13. Wall pressures in large 15° conical and pyramidal hoppers.

to bridge between the walls and would bear down on the arches below. The breaking force on the arches would therefore be greater than their own weight.

5.1 *Case 1. Rough or shallow plane-walled wedge-shaped hopper*

Considering the arch shown in Fig. 14, the maximum span that can be bridged by the powder is that at which the weight of the powder inthe arch can just be balanced by the maximum shear that the powder can develop across the vertical faces at A and B.

The maximum shear stress that can be developed in a powder with a free surface is represented by CP in Fig. 15 since the circle centre C represents the largest stress system that can be developed in the powder at a free surface (a free surface is stress free which stipulates circle must pass through origin $\tau = 0$, $\sigma = 0$), without yielding (stipulates stress circle must lie entirely below material yield locus). This maximum shear could be acting on the vertical faces at A and B providing the walls are rough or shallow enough—see Section 5.3. Note that now we are dealing with an individual powder yield locus which represents the strength that has been developed in the powder near the hopper outlet during flow.

Now f in Fig. 15 represents the unconfined yield strength of the powder, and $CP = f/2$:

$\therefore$ at limiting span S, vertical force balance gives:-

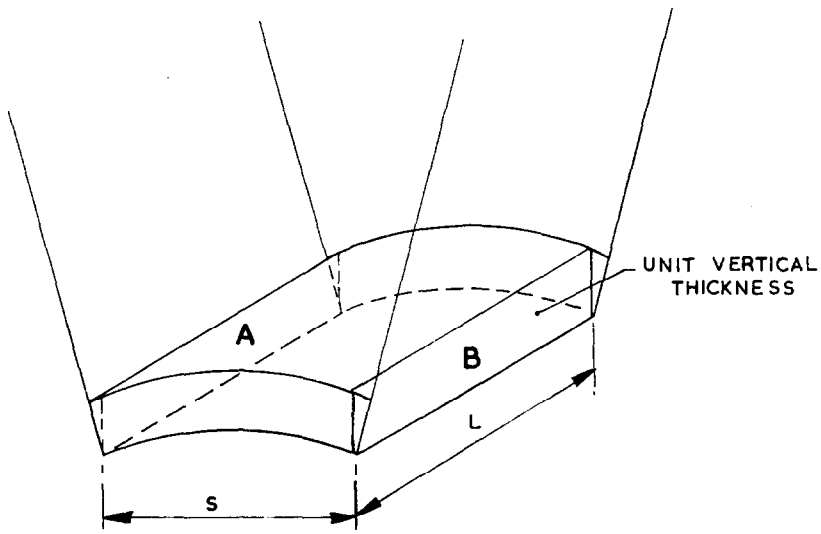

FIG. 14. The arch considered.

$$2L\frac{f}{2} = SL\gamma \quad (\gamma = \text{bulk density of powder})$$

$$\therefore S = \frac{f}{\gamma} \tag{27}$$

Since for this maximum span we required the stresses represented by point P to be those acting on a vertical face at the foot of the arch, then the major principal plane and the minor principal plane (free surface in this case) must make angles of 45° with the vertical at the foot of the arch. (This follows from the Mohr circle.)

Also, the horizontal normal stress must be constant across the arch, and the shear across any vertical surface in the arch equal to the weight of the material in that part of the arch between the

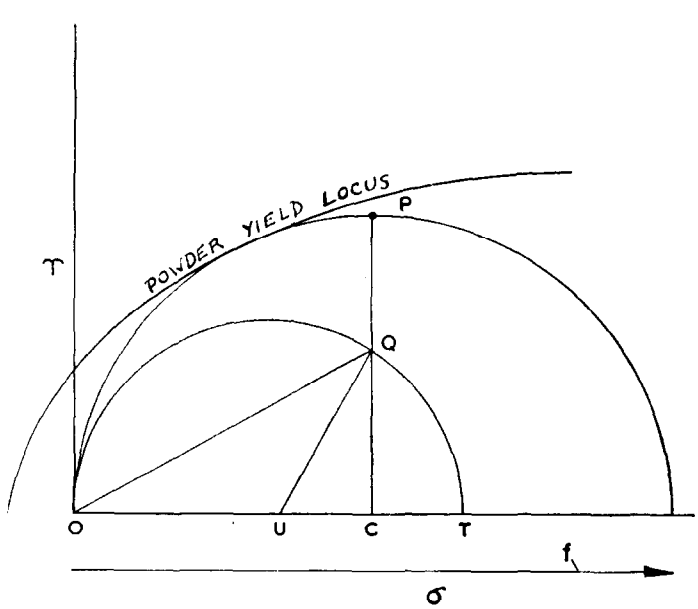

FIG. 15. Mohr circles along free arch.

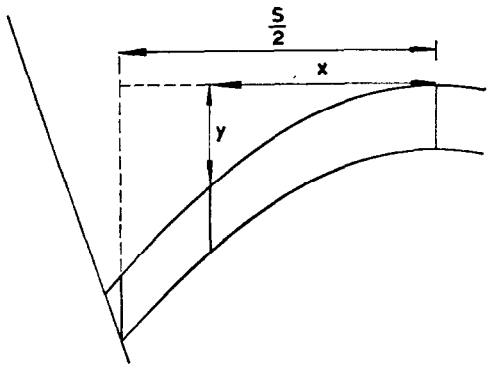

FIG. 16. Arch profile.

apex of the arch and the plane considered.

Consider a vertical plane distance x from the apex, as in Fig. 16. The shear stress on this plane is:

$$= x\gamma$$

$$= \frac{x}{S}f$$

The constant horizontal normal stress is $f/2$. Point Q (Fig. 15) represents the stress on the vertical plane considered and the Mohr circle (centre U) which passes through the origin O (since there is a free surface) and the point Q, represents the stresses in all directions in the arch at distance x from the apex. The direction of UQ on the Mohr circle diagram represents the vertical direction, the direction UO represents the direction of the minor principal plane, i.e. the free surface.

The real angle between the free surface and the vertical is therefore $\frac{1}{2}OUQ$ (Mohr circle angles are double real angles)—the real angle between the free surface and the horizontal is $\frac{1}{2}QUT$, i.e. QOT now

$$\tan \widehat{QOT} = \frac{QC}{CO} = \frac{(x/S)f}{f/2} = \frac{2x}{S}$$

The equation of the free surface is therefore

$$\frac{dy}{dx} = \frac{2x}{S}$$

$$y = \frac{x^2}{S} \tag{28}$$

The free arch is therefore of parabolic shape in this limiting case.

5.2 *Case II. Rough or shallow conical hopper*

This is similar to the above case except that now the force balance becomes:

$$2\pi R\frac{f}{2} = \pi R^2\gamma$$

and the limiting radius of the circular-sectioned outlet across which an arch can form becomes:

$$R = \frac{f}{\gamma} \tag{29}$$

The profile of the arch is again parabolic if it is assumed that the horizontal stress is constant.

5.3 *Case III. Steep smooth-walled hoppers (wedge and conical)*

In this case the width of the outlet that can be spanned is reduced because of the limited shear that can be taken by the walls. Consider the powder (with a free surface) about to fail within itself at the wall—the Mohr circle representing the stress system as shown in Fig. 17, by a circle centre C passing through O, the origin, and touching the powder yield curve.

Now the maximum shear that can be taken by the powder at the wall, in the plane of the wall is ST. The maximum shear that can therefore exist across the vertical perimeter surface is represented by UV in the Mohr circle diagram Fig 17, where UOS is α, the angle of inclination of the wall with the vertical.

$$UV = CU \sin UCV = \frac{f}{2}\sin 2(\alpha + \phi)$$

This means the limiting spans previously found for the rough or shallow-walled cases considered in Cases I and II, are reduced in the present case by a factor $\sin 2(\alpha + \phi)$ if $(\alpha + \phi)$ is less than 45°. Limiting span for plane-walled wedge hopper outlet

$$S = \frac{f}{\gamma}\sin 2(\alpha + \phi) \tag{30}$$

Limiting radius for circular outlet

$$R = \frac{f}{\gamma}\sin 2(\alpha + \phi) \tag{31}$$

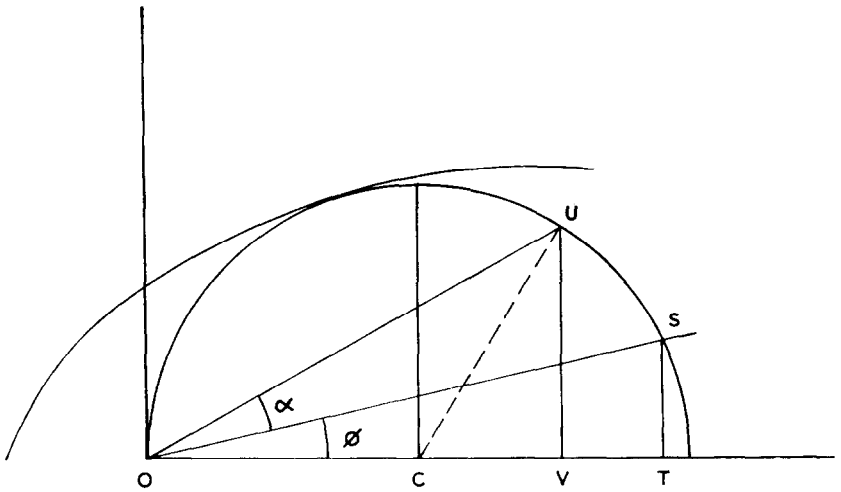

FIG. 17. Mohr circle for weak wall conditions.

Reduced openings are therefore possible with steep smooth-walled bunkers and the size of the opening approaches zero as $(\alpha + \phi)$ approaches zero. The formulae are also applicable to vertical ($\alpha = 0$) and divergent chutes (α negative). For vertical chutes the equations give "upper bound" cases of RICHMOND and GARDNER [8].

The profile of the arch is still parabolic but the slope with the horizontal at the wall is now $\alpha + \phi$ instead of 45° as previously.

In general a wall will reduce the size of the critical opening when it becomes sufficiently steep so that $(\alpha + \phi)$ is less than 45°, and this reduction is continued as the wall becomes more vertical.

Theoretically the keying of the foot of a potential arch can also be weakened by a very *shallow* smooth wall because the foot would then tend to slip outwards away from the outlet. In practice, however, this outward slip would be prevented by surrounding material and so this case has not been considered.

6. ARCHING AND FLOW FACTORS

6.1 *Vertical pipe*

The material in a pipe of, for example, circular cross-section, radius R, will not be capable of arching if it has not developed a certain strength given by:

$$f = \frac{R\gamma}{\sin 2\phi}$$

(from (31) putting $\alpha = 0$. If $\phi \geqq 45°$ then $\sin 2\phi$ to be taken as unity).

Since the material flowfactor is defined as $FF = \sigma_1/f$, and the major principal, or consolidating stress (σ_1) in the vicinity of the wall is approximately $\bar{V}$ (both being slightly greater than V_w), the critical flowfactor, which is that value which the material flowfactor must exceed to ensure no arching, is given by

$$FF_c = \frac{\bar{V} \sin 2\phi}{R\gamma} \tag{32}$$

Now in a deep circular cross-section pipe

$$\bar{V} = \frac{R\gamma}{2BD}$$

$$\therefore FF_c = \frac{\sin 2\phi}{2BD} \tag{33}$$

Values of BD were given previously in Table 1. In the case of a very rough walled pipe with a material of internal angle of friction δ of 50°,

$$\phi \to 50°, \quad BD = 0{\cdot}189, \quad FF_c = 2{\cdot}6$$

For similar material in a smooth-walled pipe, of, say, $\phi = 10°$, then $BD = 0{\cdot}022$. $FF_c = 7{\cdot}8$.

The critical flowfactor is surprisingly high for the smooth-walled pipe.

It would at first appear that cohesive material is more likely to arch in a smooth-walled pipe than in a rough pipe, and also that the likelihood of arching is independent of pipe radius. This, however, finally depends on the strength–stress curve of the material because cohesive materials have higher (more desirable) material flowfactors at higher consolidating pressures (Fig. 4 shows a typical strength–stress curve). This material characteristic would certainly mean that larger radiused pipes are less likely to arch because of the higher pressures developed. Although pressures are also higher in the smooth-walled pipe, nevertheless, an unlikely increase of material flowfactor from 2·6 to 7·8 for a corresponding pressure increase in the ratio 0·02 to 0·19 would be necessary to stop the rough-walled pipe appearing to have an advantage over the smooth.

The undesirably high critical flowfactors obtained in this section (Table 1) for vertical pipes would probably only apply in practice if there were some restriction (however slight) in the pipe. For a perfectly parallel-walled pipe the relatively high strength of the powder (especially in the very smooth-walled pipe) would never become apparent because the powder compact would be extruded *en bloc* without requiring failure within the compact.

6.2 *Convergent hoppers*

Consider a circular cross-section of radius R of a conical hopper, although exactly the same results would be obtained for a square pyramid hopper if R is half the width of the side at the section considered.

Material will be incapable of arching across the walls unless

$$f = \frac{R\gamma}{\sin 2(\alpha + \phi)} \quad \text{(from Eq. (31))}$$

Now during mass flow the major principal stress (the consolidating stress) at the section radius R was given by (25) to be

$$\sigma_1 = XY.\, R\gamma$$

The material can just arch if it develops the re-required f when flow-consolidated at this given σ_1. Since the material flowfactor is defined as $FF = \sigma_1/f$, then the critical flowfactor, which is the value that the material flowfactor must be greater than to ensure no arching in the particular hopper is

$$FF_c = XY \sin 2(\alpha + \phi) \tag{34}$$

For a given material, with constant coefficients of effective internal and wall friction, any hopper has a unique critical flowfactor which is a *constant* for that hopper. Now if the material also had a *constant* factor and this material flowfactor was greater than the critical flowfactor, no arching could occur; whilst if the material flowfactor was less than the critical flow factor arching could occur at any level; in either case the outlet size is not significant.

In practice, however, results obtained from the Jenike and annular ring shear cells indicate that the "flowfactor" for cohesive materials is not constant but generally increases with consolidating stress. In this case a critical outlet size can be calculated.

Figure 18 illustrates a case where the material characteristic lies in part above and part below a critical hopper flowfactor locus (FF_c).

When the material characteristic lies *below* the hopper FF_c locus in the graph, then the material flowfactor (σ_1/f) is desirably *high*, but when the material characteristic is above the FF_c line its flowfactor is less than FF_c and arching can occur. If we let the critical value of f at the crossover point be A, then to ensure no arching the outlet of the hopper should be of radius R_o such that

$$R_o \geqq \frac{A \sin 2(\alpha + \phi)}{y}$$

this follows from (31) remembering the sine function should only be included when $\alpha + \phi < 45°$.

The FF_c value obtained from (34) is in a sense an inverse figure of merit for a hopper system—it is the minimum flowfactor *required* from the material for mass flow to continue free from arching. The higher the FF_c of the hopper (for a given δ) the more free flowing the material is required to be to ensure no arching will occur. High material flowfactors but low hopper critical flowfactors (FF_c) are desirable.

To assess the comparative merits of different hoppers, the values of FF_c obtained for a given material ($\delta = 50°$ is taken as being of the order

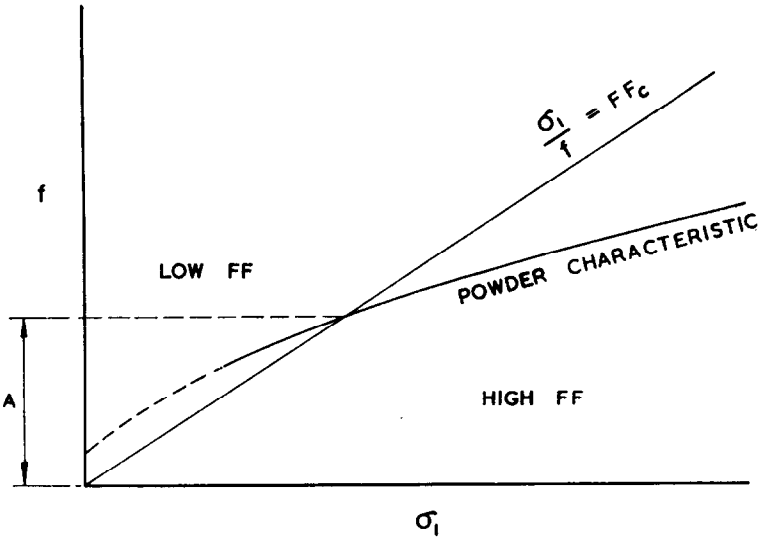

FIG. 18. Flow factor characteristics.

measured for fine coals) are calculated for various wall slope angles α (half-apex angle) and various wall friction angles ϕ and are given in Table 2.

From the figures presented in this table and other figures computed for other angle combinations, a critical flowfactor contour chart is presented in Fig. 19, together with Jenike's published contour chart. The difference is mainly due to present inclusion of the arch wall-slip factor $\sin 2(\alpha + \phi)$.

Both charts show that hoppers should generally be reasonably smooth and steep. To handle a material with a flowfactor of 2 (say), the sum of the hopper angle and wall friction angle should be less than about 45°. To handle materials with lower flowfactors the theories differ in that, whereas Jenike recommends hopper systems towards the outside of the permissible area in the chart, the present theory recommends the steepest, smoothest possible hopper.

The critical flowfactors for a wedge hopper (two plane converging walls) can be derived by a similar method to that followed for the conical hoppers. Equation (22) still applies towards the base of deep hoppers $\bar{V} = \dfrac{\gamma h}{C - 1}$ but now $C = \dfrac{BD}{\tan \alpha}$. Wedge critical flowfactors are slightly higher than the conical in the simple $D = 1$ case.

The fact that D is really greater than 1 makes very little difference to the resulting critical flowfactors. In the extreme, if $D \to \infty$, the critical flowfactors would be little affected for the steeper smoother hoppers but would increase rather more slowly with increasing hopper angle and wall friction values. The simple case gives values on the safe side. The limiting ($D \to \infty$) case gives

$$FF_c = \frac{1 + \sin \delta}{2 \sin \delta \sin 2(\alpha + \beta)} \sin 2(\alpha + \phi)$$

The first part of this equation (we know the arch wall slip factor $\sin 2(\alpha + \phi)$ is ignored) closely approximates to the whole of the published JENIKE [1] flowfactors for both wedge and conical hoppers for all materials, from $\delta = 30°$ to $\delta = 70°$ except for the rather impracticable shallow angled wedge hoppers.

6.3 *Experimental arching tests*

Fine coal (pass $\frac{1}{32}$ in. sieve) at various moisture content levels has been tested for flow characteristics in small model (1 cwt capacity) hoppers, and coal (pass $\frac{1}{8}$ in.) has just been tested in larger experimental (3 ton capacity) hoppers. The procedure here was to slowly increase the moisture content of the coal and observe its flow through different hoppers which included 3°, 15° and 30° conical and 15° and 30° pyramid with rough and smooth walls. When arching occurred the hopper outlet size was

Table 2. Constants and critical flow factors for conical or pyramidal hoppers (for material $\delta = 50°$)

α *Hopper half-apex angle°*	ϕ *Wall friction angle*	B *Eq.* (14)	C *Eq.* (18)	X *Eq.* (24)	Y *Eq.* (23)	$\sin 2(\alpha + \phi)$ *Arch wall-slip factor*	XY *Stress level Eq.* (25)	FF_c *Critical flow factor Eq.* (34)
† 0	0	0	∞	7·55	∞	0	∞	1
† 0	10	1·02	∞	5·98	0·49	0·34	2·93	1·01
† 0	20	1·18	∞	3·73	0·42	0·64	1·58	1·02
† 0	30	0·97	∞	2·36	0·52	0·87	1·22	1·06
† 0	40	0·69	∞	1·61	0·72	0·98	1·16	1·14
† 0	50	0·31	∞	1·11	1·60	1·00	1·78	1·78
15	0	1·14	8·50	5·25	0·50	0·50	2·61	1·30
15	10	1·13	8·42	3·27	0·50	0·77	1·64	1·26
15	20	0·91	6·76	2·15	0·65	0·94	1·39	1·31
15	30	0·66	4·92	1·54	0·95	1·00	1·47	1·47
15	40	0·42	3·13	1·21	1·76	1·00	2·13	2·13
30	0	1·08	3·74	2·86	0·63	0·87	1·81	1·57
30	10	0·84	2·90	1·94	0·91	0·98	1·77	1·74
30	20	0·60	2·08	1·45	1·60	1·00	2·32	2·32
30	30	0·39	1·35	1·18	5·15	1·00	6·08	6·08
45	0	0·77	1·54	1·77	1·87	1·00	3·31	3·31
45	10	0·54	1·08	1·36	11·80	1·00	16·00	16·00

† Values for $\alpha = 0$ are included to show the limits the factors are approaching as α approaches zero. $\alpha = 0$ is no longer a convergent system and the figures are not valid for vertical walled pipes.

increased by removing the lower section, and the programme continued.

Shear strength characteristics of the coal as measured on a ring shear cell so far indicate arching outlet sizes for the larger capacity hoppers in approximate accord with the present theory, whilst both hopper sets confirmed that the very steep smooth hoppers (3° half-apex angle) were best for handling the wet coal.

It is hoped to publish the full results soon.

7. Discussion

Formulae have been derived which give the range of pressures to be expected throughout any hopper (providing it is steep and smooth enough to give mass flow: see below) or vertical pipe. Other formulae have been given for deciding whether the hopper system is liable to block through arching of the powder across the outlet.

There is one factor appearing in these formulae which has not been rigidly specified—this is D, the ratio of the vertical stress near the wall to the average vertical stress over any horizontal cross section, but theory and practice so far indicate that D can be taken as unity. Assuming the horizontal stress across any level is sensibly constant (this seems reasonable because the total horizontal force on the walls and the vertical centre plane for slot section pipes or wedge hoppers, at least, must be constant; and in two axial symmetric cases, for example, the triaxial test specimen and an elastic disc, radial compresive stress is accepted as constant throughout) then D for the pipe is slightly less than unity, and for the convergent hoppers greater than unity. This is supported by some experimental results and, for hopper outlets, by Jenike's exact theory. For hoppers it has now been shown that since D is not less than unity, the "simple case" of taking D as unity is probably adequate because wall stresses are reasonably insensitive to great variations of D from unity to infinity. The latter extreme has also been studied as the "limiting case".

Pressures measured on a small model bunker and larger experimental hoppers have so far agreed reasonably well with those predicted by the theory, taking D as unity. More rigorous tests are now being carried out at these laboratories. It is unfortunate for the bunker constructor that during filling high pressures are developed near the base

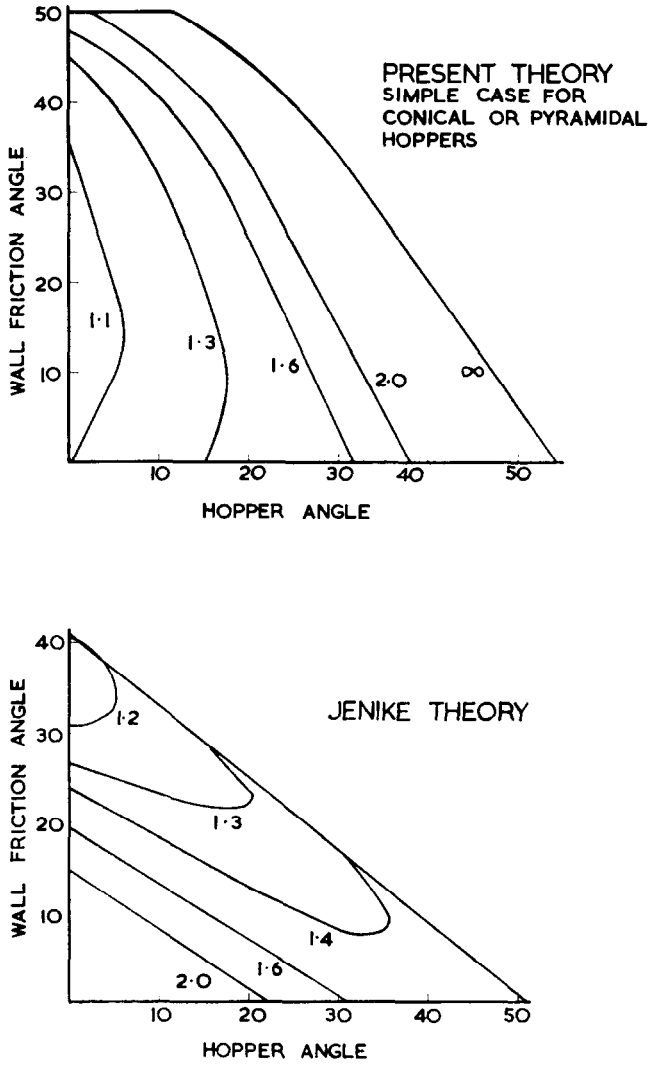

FIG. 19. Critical flow factor charts. Material $\delta = 50°$ conical hoppers.

of a bunker whilst during discharge high pressures are developed nearer the top, so that the bunker must have a high overall strength to meet both contingencies.

In the derivation of critical flowfactors a factor $\sin 2(\alpha + \phi)$ has been included to allow for the inability of a smooth steep wall to support the widest potential material arch. JENIKE [1] ignores the "weak wall" limitation on the assumption that the wall might be locally roughened. The dismissal of weak wall considerations then gives a safety factor. The case being studied, however, is a powder-hopper system which is just arching over a considerable depth (for the breaking force on the arches has been taken as being their own weight only and has not included any extruding pressure from above) and if "roughening" is introduced to support wall stresses it must also be introduced over a considerable depth; this would then be equivalent to a rough walled hopper outlet section and result in different consolidating stresses. If the wall has been considered smooth in deriving the stress field, it should surely still be considered smooth in considering the potential static arches.

Apart from the wall slip factor, the remainder of the critical flowfactor expression, i.e. XY, gives the ratio of σ_1 (major consolidating stress) to $R\gamma$ (hopper radius times material bulk density). In the limiting case XY closely approximates to the whole of Jenike's published flowfactors for wedge and conical hoppers for all materials apart from the rather impracticable shallow wedge hoppers. The simple case appears to give design data on the safe side.

What has not become apparent from our simple treatment is the outer limit of α (hopper angle) and ϕ (wall friction) for mass flow conditions. Jenike's critical flowfactor maps are limited by a cut-off which comes about because, for some obscure reason, his radial stress fields are only soluble inside this limit. The limit is lenient for the wedge hoppers ($\alpha + \phi = 90°$), but is much more stringent for the conical hoppers, being closer to $\alpha + \phi = 45°$. The present simple theory gives no sharp cut-off, although the critical flowfactors start increasing rapidly, with high ($\alpha + \phi$) values. With the inclusion of the weak wall factor the lowest critical flowfactors are for the steepest smoothest hoppers, see Fig. 19, and the position of the outside limit for mass flow is less significant than in the case of Jenike (modified chart *REF* [9] is shown), where the lowest critical flowfactors occur just on his limit for mass flow for conical hoppers.

The implication that the smoother and steeper the hopper the better its handling characteristic is in agreement with our hopper tests and with those reported by WOLF and HOHENLEITEN [10]. In addition, since the theoretical best hopper is one whose critical flowfactor is always just below the appropriate material flowfactor, then on the present theory it will probably have smooth walls which get steeper towards the outlet. This is because:

(a) stress (during flow) decreases towards the outlet,

(b) material flowfactor generally decreases with decreasing stress, and

(c) hopper critical flowfactor (on the present theory) decreases with steepening walls.

Hoppers with steepening outlets have been reported to have good handling characteristics. For example, the so-called hyperbolic outlet of YEE LEE [11] has been reported effective at three British generating stations (MADDOCKS and SMITH [12]) and a similar shape has been recommended by RICHMOND [13] from the results of theory and model hopper experiments. GARDNER [14] also makes out a theoretical case for a similar shaped hopper, for a material which is considered to have constant unconfined yield strength.

8. CONCLUSIONS

The theory for the simple ($D = 1$) case that has been developed in this paper shows promise in that:

(a) It accounts for the material pressures so far measured in experimental hoppers and bunkers:

(b) The principal stresses predicted near hopper outlets are generally similar to those JENIKE found by rigorous solution of the radial stress field.

(c) By including the wall slip factor, the theory predicts that the smoother and steeper the hopper, the better its handling characteristics and this has been given support in practical tests.

(d) A theoretical case can be made out for the smooth hoppers with walls which steepen towards the outlet, which have received favourable reports in practice.

Acknowledgement—The author gratefully acknowledges the permission given by Mr. R. H. Coates, Regional Director, S.W. Region, Central Electricity Generating Board, to publish this paper and the help given by colleagues working with him on the coal flow project at Portishead.

NOTATION

hopper	container with converging walls from top to base
bunker	container consisting of a hopper topped with a vertical walled section
chute	similar to a pipe but not necessarily circular in cross-section.
α	hopper half-apex angle
β	angle between major principal plane and hopper wall
γ	material bulk density
δ	effective angle of internal friction of material
ε	twice angle between major principal plane and pipe wall
θ	angle between a plane and major principal plane
σ	normal compressive stress
σ_1	major principal stress, the consolidating stress in a flowing system
σ_3	minor principal stress

τ shear stress
τ_v vertical shear stress near wall
ϕ angle of material-wall friction
B τ_v/V_w } factors used to determine stress fields
C $2BD/\tan\alpha$ for cone or pyramid } factors used to determine stress fields
D distribution factor equal to $V_w/\bar{V}$ arising from non-uniform vertical stress distribution on horizontal cross section. Taking $D = 1$ is probably sufficiently accurate
f unconfined yield strength of material (varies with σ_1)
FF material flowfactor, equal to σ_1/f (varies with σ_1)
FF_c hopper critical flowfactor
h depth from free surface in pipe, or height from apex in hopper
h_o height of free surface from hopper apex
V vertical compressive stress
V_c vertical compressive stress at centre line
V_w vertical compressive stress near wall
$\bar{V}$ average vertical compressive stress over horizontal cross section
V_o superimposed vertical stress
W compressive stress normal to wall.

References

[1] Jenike A. W., Gravity flow of bulk solids, Bulletin 108, Utah University, 1961.
[2] Terzaghi, K., *Theoretical Soil Mechanics*, John Wiley, New York, 1943.
[3] Roscoe K. H., Schofield A. N. and Wroth C. P., *Geotechnique* 1958 **8** 22.
[4] Lee C. A., *Chem. Engng* 1954 **61** 181.
[5] Lee C. A., *Chem. Engng* 1963 **70** 75.
[6] Jenike A. W., *Chem. Engng* 1954 **61** 175.
[7] Lenczner D., *Concr. Constr. Engng* 1964 **59** 165.
[8] Richmond O. and Gardner G. C., *Chem. Engng Sci.* 1962 **17** 1071.
[9] Jenike A. W., Storage and Flow of Solids, Bulletin 123, Utah University, 1964.
[10] Wolf E. F. and Hohenleiten H. L., *Mech. Engng* 1948 **70** 313.
[11] Yee Lee, *Combustion* 1960 **31** 20.
[12] Maddocks C. F. and Smith F., Experiments with three dimensional laboratory bunker. CEGB N.W. R&D Research Note 1/63.
[13] Richmond O., *Mech. Engng* 1963 **85** 46.
[14] Gardner G. C., *Chem. Engng Sci.* 1963 **18** 35.

Résumé—L'auteur développe une théorie simple analysant les forces approximatives auxquelles sont soumis les matériaux granuleux ou les poudres s'écoulant dans une trêmie. Celle-ci permet de connaître les facteurs critiques assurant un écoulement gravitique continu.

Le champ de force naissant lors de l'écoulement massique, a été dérivé en considérant les forces agissant sur les couches élémentaires produites simultanément à l'intérieur de l'écoulement et sur les parois du système.

De même que Jenike, qui n'a trouvé de solution exacte qu'au problème de la force des sorties, quand on considère la partie inférieure, on suppose que la force s'exerçant sur la poudre n'est fonction que des forces locales, prépondérantes lors de l'écoulement. Il a cependant été tenu compte de la tension de surface verticale qui peut se développer à proximité d'une paroi inclinée lisse. En conséquence la solution idéale pour ces systèmes, solution déduite des caractéristiques dynamiques des matériaux est certainement de disposer des parois inclinées dont l'incinaison s'accentue au fur et à mesure que l'on s'approche de la sortie.

Zusammenfassung—Eine einfache Theorie wird entwickelt, wonach Richtwerte für die Spannungen innerhalb eines granularen Materials oder Pulver, das in Fülltrichtersystemen fliesst, sowie kritische Faktoren zur Sicherung kontinuierlicher Fallströmung, erhalten werden.

Die Spannungsfelder während der Massenströmung wurden unter Berücksichtigung der Kräfte erhalten, die auf die Elementarteilchen einwirken, welche gleichzeitig unter sich selbst und entlang der Fülltrichterwände nachgeben.

In übereinstimmung mit Jenike, der eine genaue Lösung der Spannungsprobleme einzig für die Fülltrichterausgänge gegeben hat, wird bei der Betrachtung der Verspannung angenommen, dass die Pulverstärke nur von den örtlichen Spannungen, die während der vorausgehenden Strömung vorherrschten, bestimmt wird. Nun wurde aber auch die Wirkung der begrenzten Vertikalschubspannung, die in der Nähe einer steilen, glatten Wand auftreten kann, auf die potentielle Verspannungsweite in Betracht gezogen. Demzufolge wird der ideale Fülltrichter, der auf Grund der Charakteristiken von Materialstärke und Spannungen ausgelegt worden ist, wahrscheinlich steile, glatte Wände, die nach dem Ausgang hin steiler werden, aufweisen.